The Journal of Experimental Biology 213, 172-183
Published by The Company of Biologists 2010
doi:10.1242/jeb.034389

# Molt cycle regulation of protein synthesis in skeletal muscle of the blackback land crab, *Gecarcinus lateralis*, and the differential expression of a myostatin-like factor during atrophy induced by molting or unweighting

J. A. Covi[1], B. D. Bader[1], E. S. Chang[2] and D. L. Mykles[1,*]

[1]Department of Biology, Colorado State University, Fort Collins, CO 80523 USA and [2]Bodega Marine Laboratory, University of California-Davis, Bodega Bay, CA 94923 USA

*Author for correspondence (don@lamar.colostate.edu)

Accepted 14 September 2009

## SUMMARY

**In decapod crustaceans, claw muscle undergoes atrophy in response to elevated ecdysteroids while thoracic muscle undergoes atrophy in response to unweighting. The signaling pathways that regulate muscle atrophy in crustaceans are largely unknown. Myostatin is a negative regulator of muscle growth in mammals, and a myostatin-like cDNA is preferentially expressed in muscle of the land crab, *Gecarcinus lateralis* (*Gl-Mstn*). Contrary to prediction, levels of *Gl-Mstn* mRNA decreased dramatically in both the claw closer and weighted thoracic muscles when molting was induced by either eyestalk ablation (ESA) or multiple limb autotomy (MLA). However, the effect of molt induction was greater in the claw muscle. By late premolt, *Gl-Mstn* mRNA in the claw muscle decreased 81% and 94% in ESA and MLA animals, respectively, and was negatively correlated with ecdysteroids. *Gl-Mstn* mRNA in thoracic muscle decreased 68% and 82% in ESA and MLA animals, respectively, but was only weakly correlated with ecdysteroid. Claw and thoracic muscles also differed to varying extents in the expression of ecdysteroid receptor (*Gl-EcR* and *Gl-RXR*), elongation factor-2 (*Gl-EF-2*), and calpain T (*Gl-CalpT*) in response to molt induction, but levels of the four transcripts were not correlated with ecdysteroid. The downregulation of *Gl-Mstn* expression in premolt claw muscle coincided with 11- and 13-fold increases in protein synthesis in the myofibrillar and soluble protein fractions, respectively. Furthermore, the rate of the increase in the synthesis of soluble proteins was greater than that of myofibrillar proteins during early premolt (1.4:1, soluble:myofibrillar), but the two were equivalent during late premolt. By contrast, *Gl-Mstn* mRNA increased 3-fold and *Gl-CalpT* mRNA decreased 40% in unweighted thoracic muscle; there was little or no effect on *Gl-EF-2*, *Gl-EcR*, and *Gl-RXR* mRNA levels. These data indicate that Gl-Mstn expression is negatively regulated by both ecdysteroids and load-bearing contractile activity. The downregulation of *Gl-Mstn* in claw muscle may induce the elevated protein turnover associated with remodeling of the contractile apparatus during molt-induced atrophy. The upregulation of *Gl-Mstn* in unweighted thoracic muscle suggests that this factor is also involved in disuse atrophy when hemolymph ecdysteroid levels are low.**

Key words: myostatin, muscle atrophy, protein synthesis, translation, myofibrillar protein, soluble protein, calpain, ecdysone receptor, retinoid X receptor, elongation factor 2, molting, unweighting, autotomy, eyestalk ablation, limb regeneration.

## INTRODUCTION

Skeletal muscle is a highly adaptable tissue. In mammals, muscle mass is regulated by an array of physiological and pathological conditions, such as nervous activity, hormones, passive stretching, disuse and disease (reviewed by Favier et al., 2008; Tisdale, 2009). In decapod crustaceans, skeletal muscle retains a great deal of plasticity in the adult (reviewed by Mykles, 1997), which is exemplified in a reversible atrophy that occurs under two disparate conditions. One of these is the atrophy of claw muscle as part of a developmental program leading up to ecdysis, or molting (reviewed by Mykles and Skinner, 1982a). A reduction in mass facilitates withdrawal of the large closer muscle in the propodus through the narrow basi-ischial segment at ecdysis (reviewed by Mykles, 1999). Both $Ca^{2+}$-dependent and ubiquitin-dependent proteolytic systems are elevated in atrophic claw muscle (reviewed by Mykles, 1999). Calpains (Calp) degrade myofibrillar proteins and cDNAs encoding three *G. lateralis* calpains (Gl-CalpB, -M and -T) have been characterized; eyestalk ablation causes a transient increase in Gl-CalpT and ecdysone receptor (Gl-EcR) expression (Kim et al., 2005a). An extensive remodeling of the contractile apparatus is coincident with claw muscle atrophy, but no change in fiber phenotype occurs (Ismail and Mykles, 1992; Mykles and Skinner, 1981; Mykles and Skinner, 1982b). Protein synthesis is elevated during premolt (Skinner, 1965). It is hypothesized that the resulting increase in protein turnover facilitates rearrangement of the myofilament lattice in atrophic muscle (Mykles, 1997). The fully reversible atrophy of the claw muscle during premolt is induced by elevated ecdysteroid titers in the hemolymph and does not occur in leg or thoracic muscles (reviewed by Mykles and Skinner, 1982a; Mykles, 1999). Claw and thoracic muscles express different assemblages of Gl-RXR (retinoid X receptor) isoforms, suggesting that the two muscles differ in response to ecdysteroids (Kim et al., 2005b).

Reversible atrophy of thoracic muscles occurs during intermolt in response to unweighting, which is caused by autotomy, or voluntary loss, of the associated limb in three decapod species (*Carcinus maenas* Linnaeus 1758, *Uca pugilator* Bosc 1802 and *Procambarus* spp.) (Moffett, 1987; Schmiege et al., 1992). Continued atrophy despite coordinated movement of the regenerating limb bud indicates that mass of thoracic muscles is not strictly regulated by activity. Furthermore, atrophy of thoracic muscles in response to limb autotomy does not appear to involve

ecdysteroid-dependent signaling, as precocious molting is not induced if less than five limbs are autotomized in *G. lateralis* (Skinner and Graham, 1972). Ultrastructural examination of atrophic thoracic muscle demonstrates that the reduction in fiber area is associated with disruption of sarcomere organization, loss of organelles, and increased erosion of myofilaments (Schmiege et al., 1992). This stands in contrast to the highly ordered restructuring of muscle fibers in the premolt claw (Ismail and Mykles, 1992; Mykles and Skinner, 1981), and suggests that proteolytic regulation in atrophic thoracic muscle differs from that of the claw muscle.

A myostatin-like protein is expressed in *G. lateralis* (Gl-Mstn), and may be involved in regulating muscle mass in crustaceans. Myostatin, a member of the transforming growth factor-β (TGF-β) superfamily of cytokines, is a negative regulator of muscle mass in mammals (reviewed by Lee, 2004; Rodgers and Garikipati, 2008), the function of which is conserved in at least one species of lower vertebrate (Medeiros et al., 2009). Expression in non-muscle tissues does, however, suggest a broader regulatory role for myostatin, especially in lower vertebrates (reviewed by Rodgers and Garikipati, 2008). Like other TGF-β family members, myostatin is secreted as a latent autocrine/paracrine factor, and is activated by proteolytic cleavage of the propeptide; the mature peptide binds to activin receptors in the plasma membrane as a homodimer (reviewed by Herpin et al., 2004; Lee, 2004). Activation of these serine/threonine kinase receptors initiates signaling through Smad transcription factors (reviewed by Liu, 2003; Xu, 2006) that initiate a shift in the balance between anabolic and catabolic pathways in skeletal muscle, thereby causing a net loss of muscle protein. In mammals, myostatin stimulates ubiquitin-dependent protein degradation and inhibits target of rapamycin (TOR)-dependent protein synthesis (reviewed by Matsakas and Patel, 2009; Tisdale, 2009). Fiber atrophy is induced by elevated expression of myostatin (Amirouche et al., 2009; Durieux et al., 2007; Reisz-Porszasz et al., 2003; Zimmers et al., 2002). Conversely, fiber hypertrophy is induced by reduced myostatin signaling (Magee et al., 2006; Medeiros et al., 2009; Nakatani et al., 2008; Qiao et al., 2008). The Gl-Mstn cDNA encodes a 497-amino-acid (aa) polypeptide that includes a 110-aa mature peptide domain which has 52% identity and 69% similarity to human myostatin (Covi et al., 2008b). The function of this putative crustacean myostatin is unknown, but its predominant expression in skeletal muscle of the land crab suggests a role in regulating muscle mass.

The regulatory systems responsible for inducing and reversing the atrophy of skeletal muscle in crustaceans are largely unknown. Atrophy of claw muscle during premolt is triggered by ecdysteroids, whereas atrophy of thoracic muscle during intermolt is ecdysteroid-independent and may be triggered by reduced load. The purpose of this study was to examine the role of Gl-Mstn in the atrophy of claw and thoracic muscle. We hypothesized that Gl-Mstn expression would increase in atrophic skeletal muscle, and that an Mstn/Smad signaling pathway would upregulate the expression of ecdysteroid receptor and Gl-CalpT. Expression of elongation factor 2 (*Gl-EF-2*), a 'housekeeping' gene, would not be affected. Molting was induced by eyestalk ablation (ESA) or multiple limb autotomy (MLA) (reviewed by Mykles, 2001; Skinner, 1985b). Gene expression was assessed in claw closer, weighted thoracic and unweighted thoracic muscles over the molting cycle. Transcripts for Gl-Mstn (Covi et al., 2008b), ecdysteroid receptor (Gl-EcR and Gl-RXR) (Kim et al., 2005a; Kim et al., 2005b), Gl-EF-2 (Kim et al., 2004) and Gl-CalpT (Kim et al., 2005a) were quantified by real-time reverse transcription-polymerase chain reaction (qRT-PCR). Protein synthesis was measured by incorporation of [$^{35}$S]methionine in claw closer muscle cultured *in vitro*. Protein synthesis and Gl-Mstn mRNA were inversely correlated with hemolymph ecdysteroid levels. By contrast, unweighting increased Gl-Mstn expression in thoracic muscle from intermolt animals. Regulation of muscle atrophy clearly differs between the two muscles. However, analysis of the data suggests that Gl-Mstn regulates protein turnover in molt-induced and disuse muscle atrophies.

## MATERIALS AND METHODS

### Animals and molt induction

Adult male *Gecarcinus lateralis* (Fréminville 1835) used in [$^{35}$S]methionine incorporation experiments were obtained from Bermuda and maintained as described previously (Skinner, 1962); molting was induced by MLA. Adult animals used in qRT-PCR experiments were obtained from the Dominican Republic and maintained at 22°C in 75–90% relative humidity. It is relevant to note that *G. lateralis* from Bermuda, Puerto Rico and the Dominican Republic all experience similar atrophy of claw musculature during premolt. Thus, differences between Bermuda and Dominican Republic populations are assumed to be insignificant. Intermolt animals were kept in communal (7–12 animals per cage) plastic cages lined with aspen bedding wetted with 5 p.p.t. Instant Ocean (Aquarium Systems, Mentor, OH, USA). Limb-autotomized animals were kept in individual quart size (~1 l) plastic cages lined with sand wetted with 10 p.p.t. Instant Ocean. Cages for limb-autotomized animals were shielded from room lighting with cloth, as constant darkness shortens the premolt period (Bliss and Boyer, 1964). Animals were maintained under a 12 h:12 h light:dark cycle and fed iceberg lettuce, carrots and raisins twice weekly. Animals used in qRT-PCR experiments were kept in captivity for less than 2 months prior to harvesting of tissues.

Precocious molting is induced by ESA and autotomy of at least five walking legs (reviewed by Mykles, 2001; Skinner, 1985b). Regeneration of autotomized limbs occurs in two phases: basal growth, which occurs during intermolt, and proecdysial growth (Hopkins, 1993). Progression through premolt in eyestalk-ablated and multiple limb-autotomized crabs was monitored by measuring the length of the limb regenerate at the position of the third walking leg and calculating the regeneration index [R-index; =length of regenerate×100/carapace width (Bliss, 1956)]. In *G. lateralis*, the R-index ranges between 0 and 24 (Holland and Skinner, 1976; Yu et al., 2002). Eyestalk-ablated animals missing more than three limbs by the time of dissection were not used. All eight walking limbs were autotomized for the MLA experiments, and the weighted thoracic muscle harvested in this experiment was associated with the two intact chelipeds. ESA was done as described previously (Covi et al., 2008a).

### Organ culture

Penicillin and streptomycin were obtained from Sigma (St Louis, MO, USA). All other reagents used in [$^{35}$S]methionine incorporation experiments were the same as described previously (Mykles, 1990). [$^{35}$S]methionine (specific activity ~$4.07\times10^{13}$ Bq mmol$^{-1}$) was purchased from ICN Biochemicals (Costa Mesa, CA, USA).

Autotomized claws were packed in crushed ice for 3–4 h to induce apolysis (O'Brien et al., 1986). Claw closer muscle was cultured as described previously (Mykles, 1990). Briefly, tissue was equilibrated for 30–60 min in a filter-sterilized supplemented culture medium containing 10 mmol l$^{-1}$ Hepes–NaOH (pH 7.4), 316 mmol l$^{-1}$ NaCl, 5.4 mmol l$^{-1}$ KCl, 8.8 mmol l$^{-1}$ $CaCl_2$, 6.8 mmol l$^{-1}$ $MgSO_4$, 1.0 mmol l$^{-1}$ sodium phosphate, 5.6 mmol l$^{-1}$ D-glucose, 13.6 mmol l$^{-1}$ sodium citrate, 1.0 mmol l$^{-1}$ pyruvic acid, 4 mmol l$^{-1}$ glutamine, 0.2 mmol l$^{-1}$ L-alanine, 0.6 mmol l$^{-1}$ L-arginine, 0.34 mmol l$^{-1}$ L-asparagine, 0.3 mmol l$^{-1}$ aspartic acid, 0.1 mmol l$^{-1}$ L-cystine,

0.3 mmol $l^{-1}$ L-glutamic acid, 0.3 mmol $l^{-1}$ glycine, 0.2 mmol $l^{-1}$ L-histidine, 0.4 mmol $l^{-1}$ L-isoleucine, 0.4 mmol $l^{-1}$ L-leucine, 0.4 mmol $l^{-1}$ L-lysine, 0.2 mmol $l^{-1}$ L-phenylalanine, 0.3 mmol $l^{-1}$ L-proline, 0.3 mmol $l^{-1}$ L-serine, 0.4 mmol $l^{-1}$ L-threonine, 0.05 mmol $l^{-1}$ L-tryptophan, 0.4 mmol $l^{-1}$ L-valine, penicillin (10 i.u. $ml^{-1}$), and streptomycin (10 μg $ml^{-1}$). After equilibration, the medium was replaced with fresh medium containing [$^{35}$S]methionine ($3.7\times10^5$ Bq $ml^{-1}$) and the culture was incubated on an orbital shaker for 12 h. Equilibration of radioactively-labeled amino acid occurs within 1 h (Skinner, 1965) (M. Haire and D.L.M., data not shown).

After incubation, tissues were frozen in liquid $N_2$ and stored at –80°C. Muscles were homogenized in 6 volumes of buffer A (20 mmol $l^{-1}$ Tris–HCl, pH 7.5; 20 mmol $l^{-1}$ KCl; 1 mmol $l^{-1}$ EDTA; 1 mmol $l^{-1}$ dithiothreitol) with a Polytron homogenizer for 30 s at high speed. The homogenates were centrifuged at 16,000 ***g*** for 20 min at 4°C. The soluble protein in the supernatant fraction was dialyzed against two 1-l changes of 20 mmol $l^{-1}$ ammonium acetate, frozen, lyophilized, and dissolved in 1–2 ml SDS sample buffer (Medler et al., 2007) at 60°C for 10–15 min. The myofibrillar protein in the pellet obtained from centrifugation was washed three times with 40 ml buffer A and extracted with five volumes 0.6 mol $l^{-1}$ NaCl and 5 mmol $l^{-1}$ sodium phosphate (pH 7.4) at 4°C for 30 min. The soluble and myofibrillar protein solutions were clarified by centrifugation at 16,000 ***g*** for 15 min at 4°C.

The filter paper disk assay (Bollum, 1968) was used to quantify the incorporation of radioactivity into protein. Protein concentration was determined by fluorescence emission spectroscopy (Avruch and Wallach, 1971). Samples (100 μg) of soluble and myofibrillar proteins were applied to 1.5–2 cm squares of 3MM paper and air dried. Filters were washed briefly in 10% trichloroacetic acid (TCA) at room temperature, washed in 5% TCA at 90°C for 15 min, rinsed in 95% ethanol at room temperature, and air dried. Filters were placed in vials containing Ecoscint O (National Diagnostics, Atlanta, GA, USA) and the radioactivity was measured with a Beckman LS 7000 liquid scintillation counter. Incorporation was expressed as nmol [$^{35}$S]Met $mg^{-1}$ protein $h^{-1}$. For autoradiography, proteins were separated using 10% SDS-PAGE (Medler et al., 2007) and exposed to X-ray film at –80°C.

### RNA isolation and quantitative real-time RT-PCR

All reagents were of molecular biology grade. Animals were anesthetized by immersion in crushed ice for 5 min prior to dissection. Claw closer and thoracic muscles were harvested within 10 min, frozen in liquid $N_2$ and stored at –80°C. Weighted and unweighted thoracic muscle was determined by the presence or absence, respectively, of the associated pereiopod. Sufficient time had elapsed after autotomy for a basal limb regenerate to have formed.

Total RNA was isolated using TRIzol reagent (Invitrogen, Carlsbad, CA, USA) according to the manufacturer's protocol. Briefly, total RNA was treated with DNase I (Invitrogen) to remove genomic DNA. After DNase treatment, total RNA was subjected to phenol:chloroform:isoamyl alcohol extraction (25:24:1), followed by precipitation of RNA to remove DNase, salts and digested DNA. Total RNA was precipitated with 1 volume of isopropanol and resuspended in 30 μl of RNA Storage Solution (Ambion, Austin, TX, USA). Nucleotide concentration was determined by absorbance at 260 nm after 1:1 dilution with Tris-EDTA (TE) buffer (Integrated DNA Technology), and 3.75 μg was used for 30 μl cDNA synthesis reaction using SuperScript III reverse transcriptase (Invitrogen) and oligo-dT(22)VN primer (50 μmol $l^{-1}$). Resulting cDNA was treated with RNase H (New England Biolabs, Ipswich, MA, USA) to remove complementary RNA.

Quantitative analysis of *Gl-Mstn* [GenBank EU432218 (Covi et al., 2008b)], *Gl-EF-2* [GenBank AY552550 (Kim et al., 2004)], *Gl-EcR* [GenBank AY642975 (Kim et al., 2005a)], *Gl-RXR* [GenBank DQ067280 (Kim et al., 2005b)] and *Gl-CalpT* [GenBank AY639154 (Kim et al., 2005a)] was conducted using LightCycler FastStart DNA Master Plus SYBR Green I reaction mix and a LightCycler 480 thermal cycler (Roche Applied Science, Indianapolis, IN, USA). Reactions consisted of 1 μl first strand cDNA, 5 μl 2× SYBR Green Master Mix, 0.5 μl each of 10 mmol $l^{-1}$ forward primer and 10 mmol $l^{-1}$ reverse primer, and 3 μl PCR-grade water. PCR conditions included an initial denaturation at 95°C for 5 min, followed by 45 cycles of denaturation at 95°C for 5 s, annealing at gene-specific temperature (Table 1) for 5 s, and extension at 72°C for 20 s. *Gl-Mstn* primers were designed using the 3′ end of the mature peptide domain (Covi et al., 2008b), and, thus, amplified all splice variants that encoded a full-length mature peptide. Primers for RXR were designed using a sequence common to all known splice variants (Kim et al., 2005b). At the end of each run, an analysis of the PCR product melting temperature was conducted. Transcript concentrations were calculated with LightCycler 480 software (Roche; version 1.2) using standards curves produced by serial dilution of purified PCR product (10 ag $\mu l^{-1}$ to 10 ng $\mu l^{-1}$). The calibrator template used to verify consistency between runs contained cDNA pooled from claw muscle, thoracic muscle, heart, hepatopancreas, eyestalk ganglia, thoracic ganglia, testis and ovary. Ecdysteroid levels in the hemolymph were quantified by radioimmunoassay as described previously (Medler et al., 2005).

### Statistical analyses

Statistical analysis was performed using JMP 5.1.2 software (SAS Institute, Inc., Cary, NC, USA). qRT-PCR data were log transformed prior to analysis to reduce differences in variance from the mean.

Table 1. Primers used for qRT-PCR

| Name | Sequence | $T_m$ (°C) | Product size |
|---|---|---|---|
| cEF2 F1 | 5′-TTCTATGCCTTTGGCCGTGTCTTCTC-3′ | 62 | 229 bp |
| cEF2 R1 | 5′-TGATGGTGCCCGTCTTAACCAGATAC-3′ | | |
| RcEcR F1 | 5′-CACGAAGAATGCCGTGTACCAGTGTA-3′ | 62 | 371 bp |
| RcEcR R1 | 5′-CATCTGCTTCAGTTGGCTGCTCAAAC-3′ | | |
| MstnIMP F2 | 5′-GCTGTCGCCGATGAAGATGT-3′ | 60 | 118 bp |
| MstnIMP R1 | 5′-GTGTGGCTAGAATGAGAGATGTG-3′ | | |
| qGl-RXR F1 | 5′-CTCAGGCAAGCACTATGGCGT-3′ | 62 | 164 bp |
| qGl-RXR R1 | 5′-TCAAGCACTTCTGGTAGCGGCAG-3′ | | |
| RcCalpT F1 | 5′-TCTCTGATGTGCTGTGCCATAACTCC-3′ | 60 | 276 bp |
| RcCalpT R1 | 5′-TGATGCAGAGACCTGTGACCATTCTG-3′ | | |

$T_m$, melting temperature.

Variances among log-transformed data were determined to be equivalent using Brown–Forsythe tests ($P$<0.05). Means for transcript abundance were compared among developmental stages for individual muscle types using analysis of variance (ANOVA). *Post-hoc* multiple comparisons were made using Tukey–Kramer HSD tests. A paired *t*-test was used to compare means for transcript abundance between claw and thoracic muscles, or weighted and unweighted thoracic muscles, at each developmental stage. All data not plotted as individual points are presented as mean ± 1 s.e.m. and the level of significance was set at $\alpha$=0.05 for all statistical analyses.

## RESULTS

### Scales for presentation of data

Data are presented as a function of three variables: time, R-index and molt stage. Time was used to describe events following ESA and ecdysis, but did not allow comparisons with premolt animals that were induced to molt by MLA. R-index was used to compare the effects of molt induction by ESA and MLA during premolt. The molt stage classifications developed by Drach (Drach, 1939), and later modified by Skinner on *G. lateralis* (Skinner, 1962), were used to integrate analyses based on time and R-index.

### Effects of molt induction by MLA on claw muscle protein synthesis

For anecdysial, or intermolt (stage $C_4$) animals, [$^{35}$S]methionine incorporation into soluble protein was 2.7-fold greater than incorporation into myofibrillar proteins (0.167 *vs* 0.063 nmol [$^{35}$S]Met mg$^{-1}$ protein h$^{-1}$; Fig. 1A; $P$<0.0001). During early premolt (R-index=8 to 13), incorporation began to increase, reaching synthetic rates for myofibrillar and soluble proteins that were 11 and 13 times greater ($P$<0.0001), respectively, by mid premolt than those in claw muscles from intermolt animals (Fig. 1A). The stoichiometry between the synthesis of soluble and myofibrillar proteins changed during the late $D_0$ stage of premolt; the synthesis of soluble protein increased at a greater rate than myofibrillar protein (1.4 to 1) during the first half of stage $D_0$, but the relative increase in synthetic rates for the two protein pools were equivalent thereafter (Fig. 1B). Slopes for linear regressions of myofibrillar and soluble synthetic rates at $R$<13 and $R$>13 are significantly different ($P$<0.05), and the synthesis of soluble and myofibrillar proteins within the same muscle was highly correlated (Fig. 1B). Overall, the synthesis of soluble protein during premolt was about 3.2-fold greater than that of myofibrillar protein (Fig. 1A).

SDS-polyacrylamide gel electrophoresis showed no quantitative or qualitative changes in the protein composition of soluble and myofibrillar preparations during premolt (Fig. 2A,B). Autoradiographs showed increased global synthesis of soluble and myofibrillar proteins (Fig. 2C,D). There were no qualitative differences in the proteins synthesized at any molt stage. Furthermore, the relative synthesis of each of the proteins in the soluble and myofibrillar fractions did not change during the premolt period (Fig. 2C,D).

### Effects of ESA and MLA on hemolymph ecdysteroids levels

Titers of hemolymph ecdysteroids increased in response to both ESA and MLA, but were higher in ESA animals at all R-index values sampled (compare Fig. 3A and Fig. 4A). ESA induced a five-fold increase in ecdysteroids over the first 24 h that was followed by a much slower and prolonged increase; by 2 weeks post-ESA, the hemolymph ecdysteroid level was 12-fold higher than that observed in intact animals (Fig. 3A; $R$=15.5). During the third week following ESA, ecdysteroids increased rapidly again, and were 32-fold greater than levels in intact animals by day 20 (Fig. 3A; $R$=19.9). The initial increase in hemolymph ecdysteroids observed in response to MLA was more gradual than that observed for ESA. Mean ecdysteroid levels were only 7-fold greater than in intact animals 45±11 days after MLA (Fig. 4A; $R$=15.1). Hemolymph ecdysteroids increased rapidly in late premolt ($R$=23.4), reaching a concentration that was 28-fold greater on average than that in intermolt animals. Ecdysteroid levels decreased to <7 ng ml$^{-1}$ in postmolt animals and remained low for at least 10 days following ecdysis (Fig. 4A).

### Effects of ESA on gene expression in claw and weighted thoracic muscles

ESA had small or only transient effects on *Gl-EF-2* expression during the first two weeks post-ESA. The copy number of mRNA transcripts for *Gl-EF-2* did not change significantly in claw muscle during the first 14 days following ESA (Fig. 3C; $R$≤17). However,

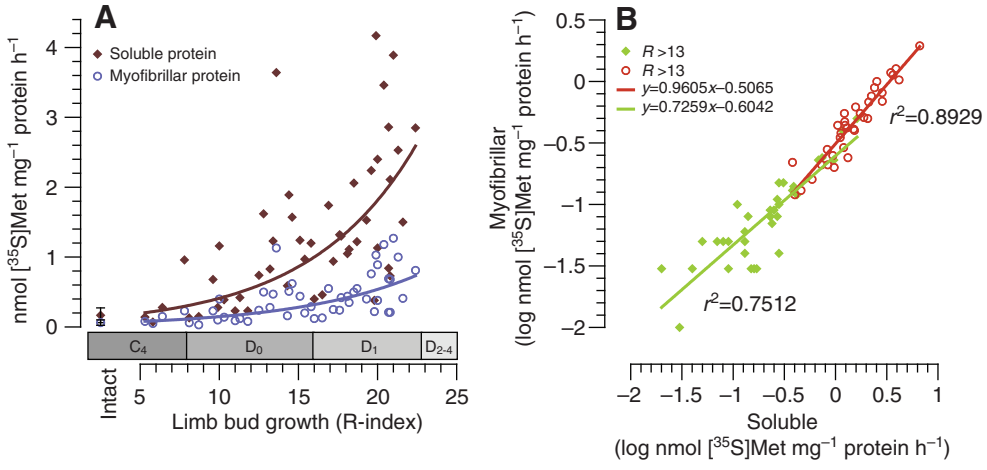


Fig. 1. Effects of molting on synthesis of soluble and myofibrillar proteins in claw muscles *in vitro*. Claw muscles from intermolt (R-index=7) and premolt (R-index=7–22) were incubated for 12 h in a medium containing [$^{35}$S]methionine; incorporation of radioactivity was quantified by the filter paper disk assay and expressed as nmol [$^{35}$S]Met mg$^{-1}$ protein h$^{-1}$. (A) Protein synthesis as a function of R-index in animals stimulated to molt by multiple leg autotomy. Best fit lines using exponential functions are shown (soluble, $r^2$=0.533; myofibrillar, $r^2$=0.480). (B) Synthesis of myofibrillar proteins as a function of the synthesis of soluble proteins. Corresponding molt stages based on epidermal changes (Drach, 1939) are given above the abscissa; correlation between Drach stages and limb regeneration is based on Holland and Skinner (Holland and Skinner, 1976) and Skinner (Skinner, 1985a).

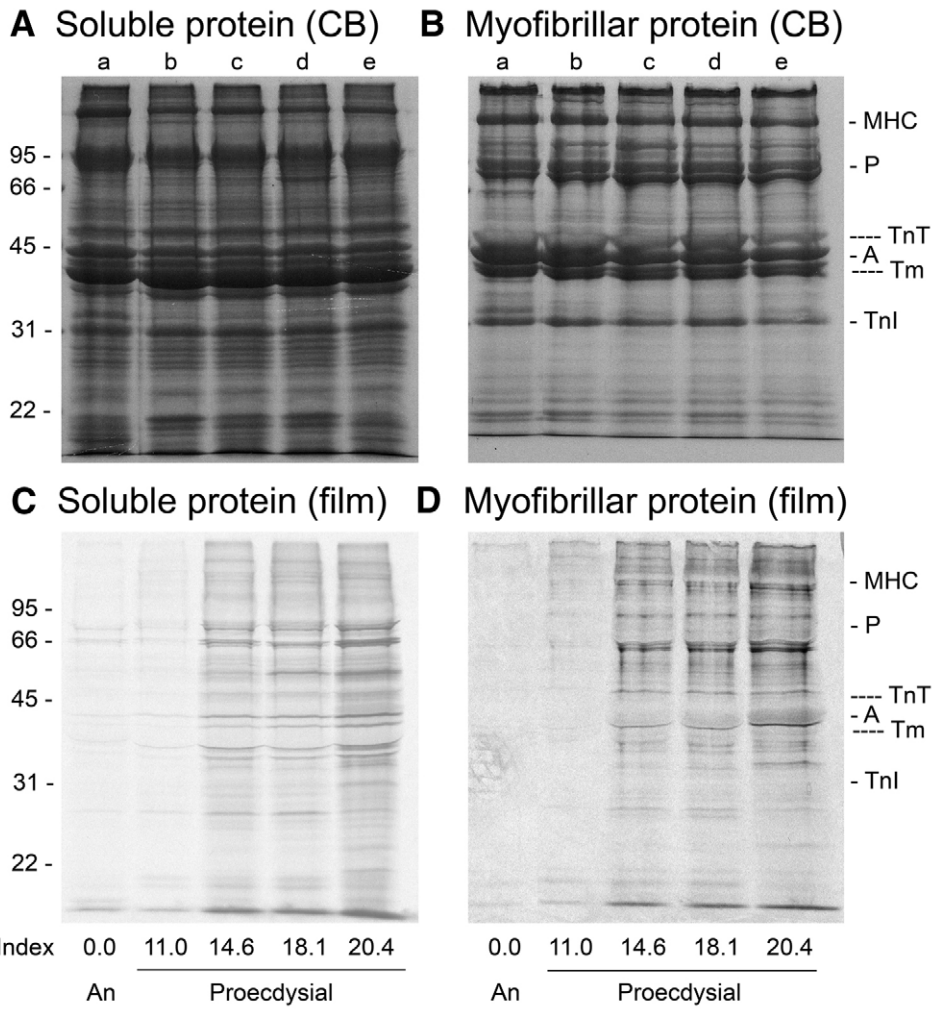


Fig. 2. Autoradiographs showing synthesis of soluble and myofibrillar proteins in claw muscles from intermolt and premolt land crabs. Muscles were incubated and processed as described in the legend to Fig. 1. Samples of soluble (60 μg; A,C) and myofibrillar proteins (50 μg; B,D) were separated on 10% SDS-polyacrylamide gels. One pair of gels (A,B) was stained with Coomassie Blue (CB); a second pair was dried and exposed to X-ray film (film) for 8 weeks (C) or 12 weeks (D). Lane a, samples from anecdysial (An), or intermolt, muscle; lanes b–f, samples from proecdysial, or premolt, muscles (R-index=11.0, 14.6, 18.1 and 20.4). A, actin; MHC, myosin heavy chain; P, paramyosin; Tm, tropomyosin; TnI, troponin-I; and TnT, troponin-T. Positions of molecular mass standards, in kDa, are indicated on the left.

by 20 days post-ESA ($R$=20), *Gl-EF-2* levels had increased 2.1-fold relative to that in intact animals (Fig. 3C). In thoracic muscle, *Gl-EF-2* copy number decreased by 35% during the first 24 h following ESA and returned to intact levels within 2 weeks (Fig. 3C). These levels are similar to previously published values (Kim et al., 2005a). Transcript copy number for *Gl-EF-2* was consistently lower in thoracic muscle than in claw muscle at all molt stages (Fig. 3C).

ESA caused a large reduction in *Gl-Mstn* expression, but the timing and extent of this reduction differed between claw and thoracic muscles. No significant change in the number of copies of *Gl-Mstn* mRNA occurred in claw muscle during the first 3 days following ESA (Fig. 3D; $R \leq 8$). However, the beginning of a downward trend in *Gl-Mstn* transcript abundance in claw muscle was apparent at day 7 post-ESA ($R$=10). By day 20 ($R$=19.9), *Gl-Mstn* transcript level had decreased by 81% (Fig. 3D). No significant change in Gl-Mstn copy number was apparent until day 20 post-ESA in thoracic muscle ($R$=19.9), and the magnitude of the decrease in copy number (68%) was smaller than that observed for claw muscle (Fig. 3D). This difference in the response to ESA is supported by statistical comparison of transcript abundance in the two muscle tissues at each molt stage; transcript copy number for *Gl-Mstn* was significantly lower in thoracic muscle in intact and early $D_0$ premolt animals ($R \leq 7.2$), but was significantly higher in thoracic muscle at $R$=15 (Fig. 3D).

Effects of ESA on the expression of the subunits of the ecdysteroid receptor (Gl-EcR and Gl-RXR) were dependent on tissue and subunit type. ESA had no significant effect on transcript abundance of *Gl-EcR* in claw muscle, but induced a steady and significant increase in thoracic muscle (Fig. 3B). By day 20 ($R$=19.9), *Gl-EcR* transcript levels had increased by 3.2-fold relative to the level in intact animals (Fig. 3B). It is relevant to note that variances around the mean for days 1 and 3 following ESA were higher relative to those at later time points and for other gene transcripts (Fig. 3). Consequently, for *Gl-EcR* trends spanning these earlier time points could be obscured by the high degree of variation among individuals during the immediate response to ESA. Copy number for *Gl-EcR* in thoracic muscle was significantly lower than that of claw muscle at low and high R-index values. Transcript copy number for *Gl-RXR* did not change significantly in claw muscle during the first 3 days following ESA (Fig. 3E; $R \leq 8$). *Gl-RXR* transcript levels dropped 51% between day 3 and 7 post-ESA ($R$=7.2 and 10, respectively), and slowly returned to normal levels thereafter (Fig. 3E). A similar trend was apparent in thoracic muscle, although the drop between day 3 and 7 post-ESA was slightly larger (65%) and the subsequent return to normal levels was not observed (Fig. 3E). It is important to note that the qRT-PCR primers amplified a region conserved among all known isoforms. Therefore, the data are the sum of all *Gl-RXR* variants, which differ in expression between claw and thoracic muscles (Kim et al., 2005b).

After a transient decrease, ESA caused a modest increase in *Gl-CalpT* expression in claw and thoracic muscles; this was followed by a decrease at later premolt stages. Transcript abundance for *Gl-*

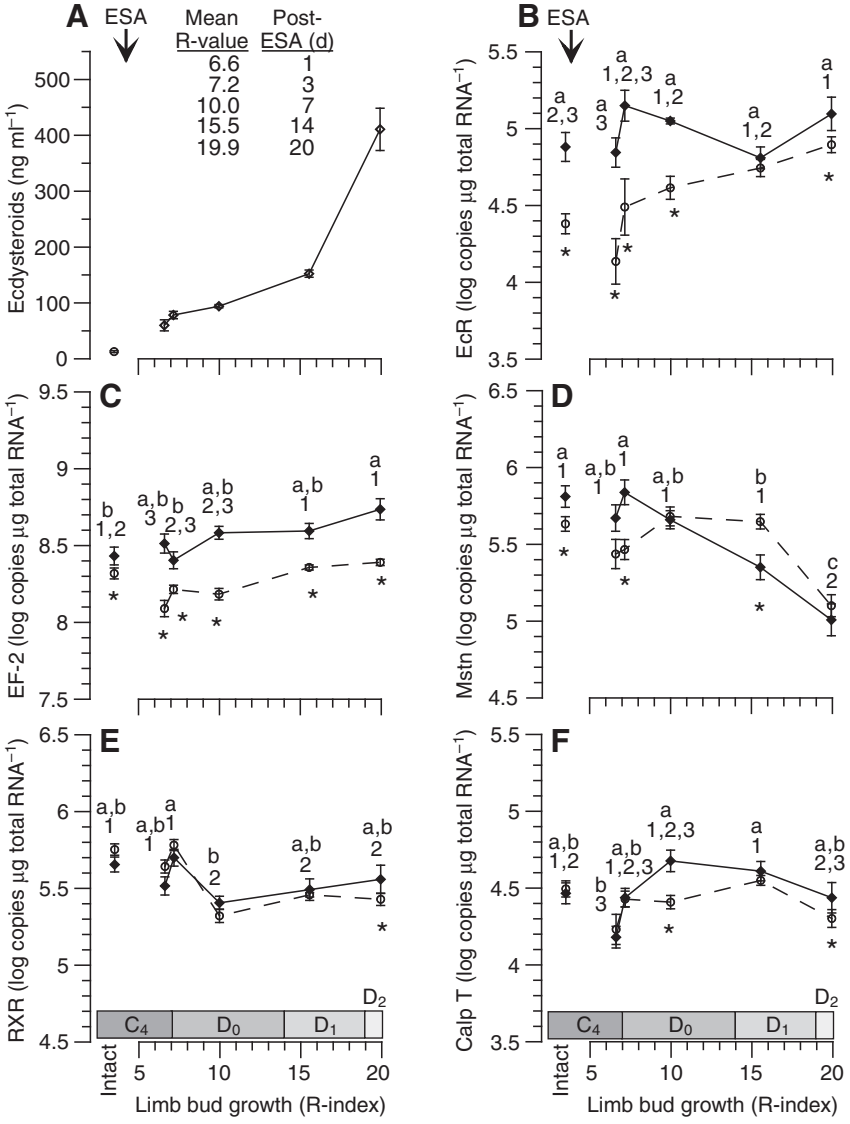


Fig. 3. Effects of eyestalk ablation on hemolymph ecdysteroids (A) and gene expression (B–F) in claw and weighted thoracic muscles. (A) Hemolymph ecdysteroid titers were quantified by radioimmunoassay. Data are expressed as a function of R-index; inset delineates the relationship between the R-index and time following ESA. Abundance of mRNA transcripts, quantified by qRT-PCR, are plotted as a function of R-index for ecdysone receptor (*Gl-EcR*; B), elongation factor 2 (*Gl-EF-2*; C), myostatin (*Gl-Mstn*; D), retinoid X receptor (*Gl-RXR*; E), and calpain T (*Gl-CalpT*; F). Intermolt animals are plotted as separate data points to the left of the R-index scale (Intact). Open circles and a dashed line, thoracic muscle; closed diamonds with a solid line, claw muscle. Standard error measurements for R-index means are not displayed, but are less than or equal to 0.3. Shared letters indicate no significant difference for multiple comparisons among claw muscle data. Shared numbers indicate no significant difference for multiple comparisons among thoracic muscle data. Asterisks indicate a significant difference between claw and thoracic muscle means at the same molt stage. Scales for ordinates are identical, but the ranges are shifted to accommodate varied levels of expression of different genes. Corresponding molt stages are given above the abscissa as in Fig. 1. Data are presented as mean ± 1 s.e.m. (*N*=11–12).

*CalpT* decreased by 40–50% during the first 24 h following ESA in both muscles, but this decrease was only statistically significant in thoracic muscle (Fig. 3F). Copy number for *Gl-CalpT* returned to the levels in intact animals in both tissues by day 3 post-ESA (*R*=7.2). Transcript levels in claw muscle increased by 2.7-fold between days 1 and 14 post-ESA (*R*=6.6 and 15.5, respectively) whereas levels in thoracic muscle increased by 1.7-fold (Fig. 3F). Transcript abundance decreased between day 14 and day 20 (*R*=15.5 and 19.9, respectively) post-ESA in both muscles, but this drop was only statistically significant in thoracic muscle (Fig. 3F).

### Effects of MLA on gene expression in claw and thoracic muscles

The expression of *Gl-EcR* and *Gl-RXR* was examined following MLA. Levels of mRNA were similar between claw and thoracic muscles at all molt stages except 10 days postmolt for both *Gl-EcR* and *Gl-RXR* (Fig. 4B,E). *Gl-EcR* transcript levels in both muscles increased by two- to threefold during premolt, decreased by 95% between late premolt and 2 days postmolt, and remained low for at least 10 days after ecdysis (Fig. 4B). No significant change in *Gl-RXR* mRNA was observed in either muscle over a molting cycle (Fig. 4E). However, levels of both *Gl-EcR* and *Gl-RXR* transcripts were significantly higher in thoracic muscle from 10-day postmolt animals (Fig. 4B,E).

In response to MLA, the abundance of *Gl-EF-2* transcripts decreased by 42% in claw muscle and 40% in thoracic muscle during the early $D_0$ stage of premolt, but this change was only statistically significant for the thoracic muscle (Fig. 4C; *R*=10). *Gl-EF-2* transcript abundance in both muscles returned to intact levels by the late $D_0$ stage of premolt (Fig. 4C; *R*=15). *Gl-EF-2* levels were generally lower in claw muscle than thoracic muscle (Fig. 4C).

Transcript abundance for *Gl-Mstn* decreased in both claw and thoracic muscle following MLA, but this decrease was more pronounced in claw muscle. This is illustrated by a direct comparison between claw and thoracic muscles at specific molt stages; *Gl-Mstn* mRNA levels for claw muscle were significantly greater than that of thoracic muscle during the early $D_0$ stage of premolt (*R*=10), but significantly less than thoracic muscle during the late $D_1$ stage of premolt (*R*=23.5) and 10 days postmolt (Fig. 4D). *Gl-Mstn* copy number in the high R-index group was 94% lower than that of intact animals for claw muscle and 82% lower for thoracic muscle (Fig. 4D; intact *vs R*=22.3). *Gl-Mstn* transcript levels increased over tenfold in claw and fivefold in thoracic muscle between late premolt (*R*=22.3) and 2 days postmolt groups (Fig. 4D). A large decrease in

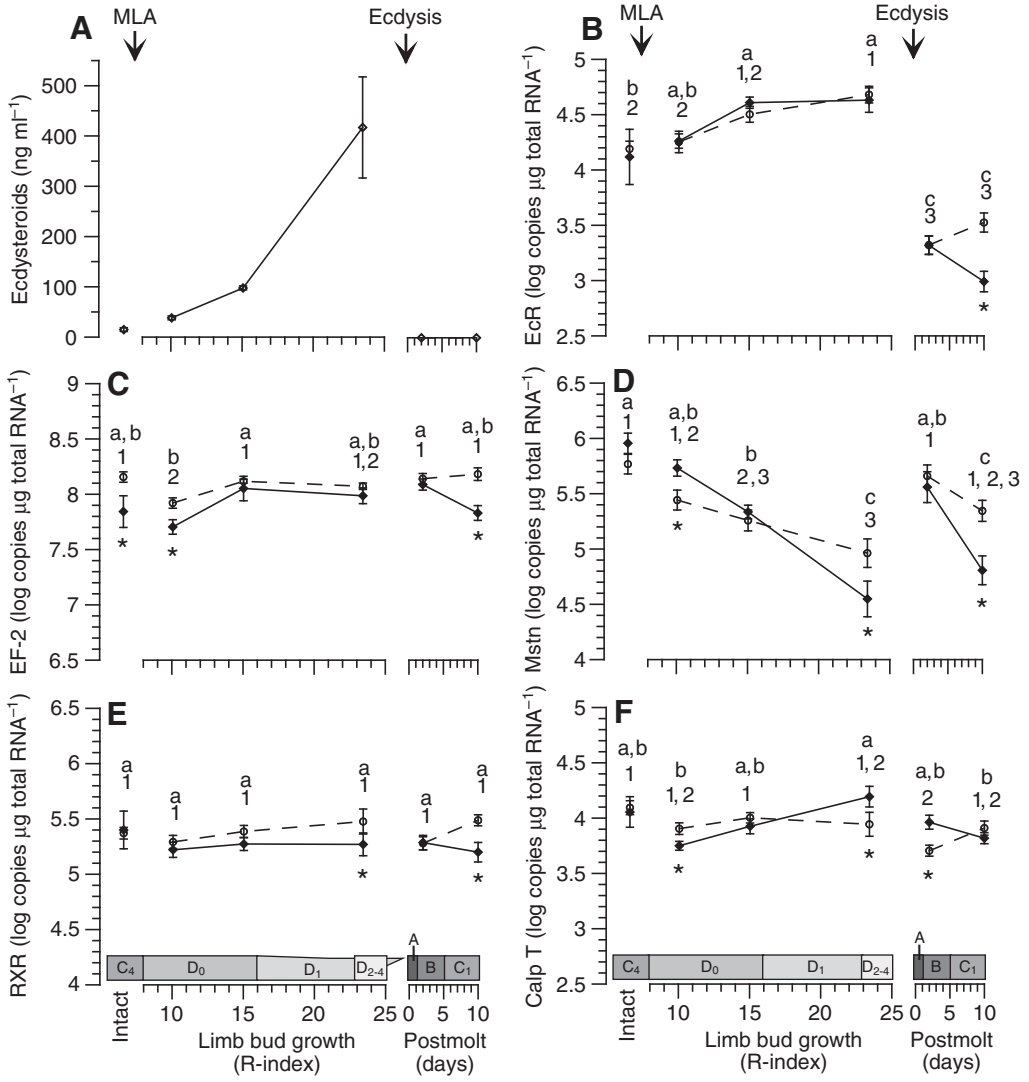


Fig. 4. Effects of multiple limb autotomy on hemolymph ecdysteroids (A) and gene expression (B–F) in claw and weighted thoracic muscles. (A) Hemolymph ecdysteroid titers were quantified by radioimmunoassay. Data are expressed as a function of R-index. Postmolt measurements of hemolymph ecdysteroids were <11 ng ml$^{-1}$; error bars for postmolt are excluded, because measurements were often below the detection limit of 5 ng ml$^{-1}$. Abundance of mRNA transcripts, quantified by qRT-PCR, for the *Gl-EcR* (B), *Gl-EF-2* (C), *Gl-Mstn* (D), *Gl-RXR* (E) and *Gl-CalpT* (F) are plotted as a function of R-index for premolt animals and days following ecdysis for postmolt animals. Data for intermolt animals are plotted separately to the left of the R-index scale (Intact). Open circles and a dashed line, thoracic muscle; closed diamonds with a solid line, claw muscle. Standard error measurements for R-index means are not displayed, but are less than or equal to 0.5. Shared letters indicate no significant difference for multiple comparisons among claw muscle data. Shared numbers indicate no significant difference for multiple comparisons among thoracic muscle data. Asterisks indicate a significant difference between claw and thoracic muscle means at the same molt stage. Scales for ordinates are identical, but the ranges were shifted to accommodate varied levels of expression among genes. Corresponding molt stages are given above the abscissa as in Fig. 1. Data are presented as mean ± 1 s.e.m. Sample sizes varied with molt stage (intact, $N$=8; $R$=10.1 and 15.0, $N$=12; $R$=23.4, $N$=9; 2 days and 10 days postmolt, $N$=14).

*Gl-Mstn* transcript abundance occurred between 2 and 10 days postmolt for both muscles; a drop of 84% occurred in claw and a drop of 57% occurred in thoracic muscle (Fig. 4D).

Changes in the abundance of *Gl-CalpT* transcripts differed between claw and thoracic muscles in response to MLA. The transcript copy number for *Gl-CalpT* transcript did not change significantly in thoracic muscle during premolt (Fig. 4F). In claw muscle, *Gl-CalpT* mRNA increased significantly during premolt; copy number at late premolt ($R$=23.5) was 3.2-fold greater than that at early premolt ($R$=10; Fig. 4F). This is supported by a comparison of claw and thoracic muscle at specific R-index values; transcript levels for claw muscle were significantly less than that of thoracic muscle during early premolt and significantly greater during late premolt (Fig. 4F; $R$=10 *vs* $R$=23.5). However, because transcript abundance decreased by 60% in claw muscle during early premolt, the late premolt value was not significantly higher than that of the intact animals.

### Relationship between *Gl-Mstn* mRNA and hemolymph ecdysteroid levels

Abundance of *Gl-Mstn* mRNA was generally correlated with circulating ecdysteroids, but this relationship was much stronger in MLA animals than in ESA animals. *Gl-Mstn* transcript abundance was high at low ecdysteroid levels, and decreased significantly as ecdysteroid titers increased during premolt (Fig. 5). *Gl-Mstn* mRNA in claw muscle was negatively correlated with

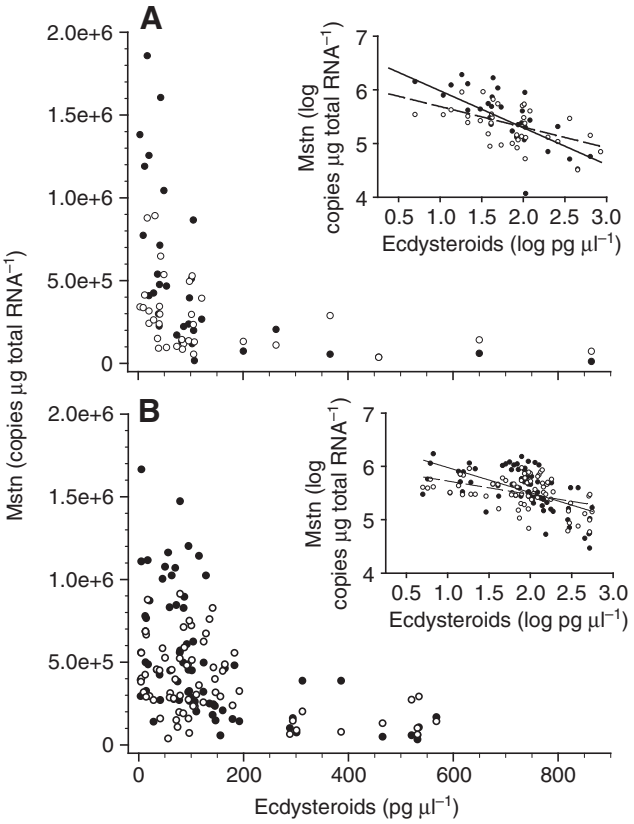


Fig. 5. Relationship between *Gl-Mstn* mRNA and hemolymph ecdysteroid levels. Regressions of *Gl-Mstn* transcript abundance *vs* ecdysteroid titers include all intermolt and premolt data used in Fig. 3D and Fig. 4D. Animals were stimulated to molt by MLA (A) or ESA (B). Log transformed data are plotted in the insets. Open circles and dashed line, thoracic muscle; solid circles and solid line, claw muscle. Correlation coefficients for linear regressions in insets are as follows: (A) claw muscle, $r^2$=0.6221; thoracic muscle, $r^2$=0.2725; (B) Claw muscle, $r^2$=0.3419; thoracic muscle, $r^2$=0.1834.

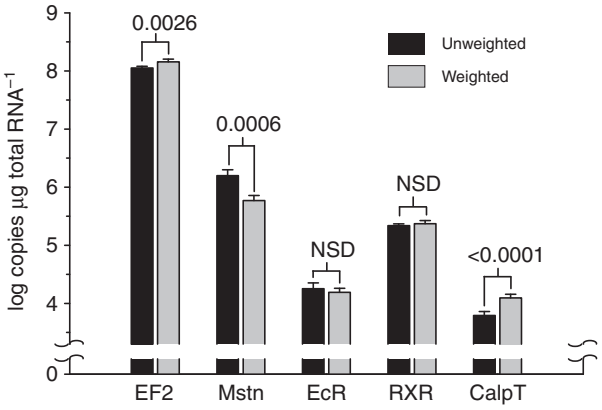


Fig. 6. Effects of unweighting on gene expression in thoracic muscle of intermolt land crabs. Comparison of *Gl-EF-2*, *Gl-Mstn*, *Gl-EcR*, *Gl-RXR* and *Gl-CalpT* transcript abundance between unweighted (black) and weighted (gray) thoracic muscles from the same animals. Data presented as mean ± 1 s.e.m.; *N*=6. *P*-values for significant differences are given above each pairwise comparison; NSD, no significant difference at $\alpha$=0.05.

hemolymph ecdysteroids in animals induced to molt by MLA (Fig. 5A inset). A similar relationship was evident in ESA animals, but variability was much higher at ecdysteroid levels between 50 and 200 pg µl$^{-1}$ (Fig. 5B) and levels of *Gl-Mstn* mRNA were weakly correlated with hemolymph ecdysteroids (Fig. 5B inset). If intact animals were excluded from the analysis, the correlation coefficient for a linear fit to the log *vs* log data for ESA claw muscle increased to 0.720, whereas the fit for thoracic muscle did not change appreciably (data not shown). The negative correlation between hemolymph ecdysteroids and Gl-Mstn mRNA was weaker for thoracic muscle than claw muscle in both MLA and ESA experiments (Fig. 5A,B insets). Expression of Gl-EcR, Gl-RXR. Gl-CalpT, and Gl-EF-2 was not correlated with ecdysteroid concentration (data not shown).

### Effects of unweighting on gene expression in thoracic muscle

Limb autotomy induced specific changes in gene expression in the corresponding thoracic muscle of intermolt animals. Unweighting had little or no effect on expression of *Gl-EF-2*, *Gl-EcR* and *Gl-RXR* in thoracic muscle (Fig. 6). However, transcript levels of both *Gl-Mstn* and *Gl-CalpT* were significantly altered in response to unweighting; *Gl-Mstn* mRNA increased threefold, whereas *Gl-CalpT* mRNA decreased by more than 40% (Fig. 6). Abundance of *Gl-Mstn* mRNA in unweighted thoracic muscle paralleled *Gl-Mstn* mRNA abundance in weighted thoracic muscle during premolt and postmolt (Fig. 7).

## DISCUSSION

The primary goal of the present study was to assess the role of a myostatin-like protein, Gl-Mstn, in regulating the atrophy of claw closer muscle during premolt and thoracic muscle after limb autotomy. The data show that (1) protein synthesis in claw muscle increases in two distinct stages during premolt; (2) transcript level for *Gl-Mstn* decreases dramatically in skeletal muscles during both premolt and postmolt; (3) transcript level for *Gl-Mstn* in atrophic claw muscle is negatively correlated with hemolymph ecdysteroids during premolt; (4) transcript level for *Gl-Mstn* in intermolt animals is significantly elevated in unweighted thoracic muscles; and (5) transcript levels for *Gl-CalpT*, *Gl-EF-2*, *Gl-EcR*, and *Gl-RXR* in skeletal muscle are not correlated with *Gl-Mstn* transcript abundance or hemolymph ecdysteroids. Together these data provide evidence supporting the hypothesis that Gl-Mstn mediates reversible atrophy of skeletal muscle in response to elevated ecdysteroids and unweighting, but through two distinct mechanisms.

Skeletal muscle mass is determined by the balance between protein synthetic and degradation rates. In general, muscle atrophy results from the net loss of protein caused by increased protein degradation, decreased protein synthesis, or a combination of the two (reviewed by Sandri, 2008; Tisdale, 2009). The large increase in protein synthesis that occurs in the claw during molt-induced atrophy is an exception to this rule, as protein degradation must increase to an even greater extent to effect the reduction in mass that occurs during the premolt period. This seems counter-productive, especially in consideration of the increased energetic costs associated with upregulated anabolic processes. In mammals, increased protein turnover occurs during remodeling of skeletal muscle undergoing fiber transformation and cardiac muscle undergoing rosiglitazone-induced hypertrophy (Festuccia et al., 2009; Termin and Pette, 1992). We suggest that increased protein turnover is necessary for the extensive remodeling of the sarcomere that is observed as myofibrils are reduced in size (Mykles, 1997). In the isomorphic claws of land crab, *G. lateralis*, and the major claw of fiddler crab, *Uca pugnax*, there is a preferential loss of about 11 thin myofilaments for every thick myofilament, which results in

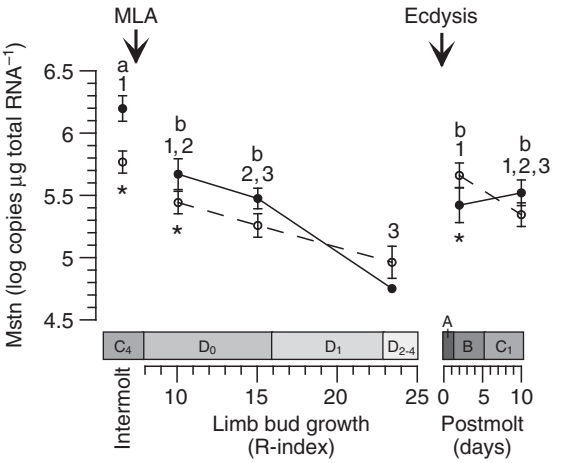


Fig. 7. Effects of molting on *Gl-Mstn* expression in weighted and unweighted thoracic muscles. Abundance of *Gl-Mstn* mRNA transcripts is plotted as a function of R-index for premolt animals and days following ecdysis for postmolt animals. Molting was induced by MLA.Data from intermolt animals are plotted as separate points to the left of the R-index scale (Intermolt). This is the same intermolt data as in Fig. 6. Open circles and a dashed line, weighted thoracic muscle; this is the same data as in Fig. 4D. Closed circles and a solid line, unweighted thoracic muscle. Standard error measurements for R-index means are not displayed, but are less than or equal to 0.5. Shared numbers indicate no significant difference for multiple comparisons among weighted muscle data. For unweighted muscle data different letters indicate a significant difference for multiple comparisons. Asterisks indicate a significant difference between unweighted and weighted thoracic muscle means at the same molt stage. Corresponding molt stages are given above the abscissa as in Fig. 1. Data are presented as mean ± 1 s.e.m. Sample sizes varied with molt stage (intact, $N$=8; $R$=10.1 and 15.0, $N$=12; $R$=23.4, $N$=9; 2 days and 10 days postmolt, $N$=14) Only one measurement was made for the unweighted group during late premolt.

a decrease in the thin:thick myofilament ratio from ~9:1 to ~6:1; this corresponds to a 31% to 64% decrease in the ratio of actin to myosin heavy chain (Ismail and Mykles, 1992; Mykles and Skinner, 1981; Mykles and Skinner, 1982b). The loss of thin myofilaments increases the thick myofilament packing density between 51% and 72% (Ismail and Mykles, 1992; Mykles and Skinner, 1981). It is generally thought that exchange of myofibrillar proteins between sarcomeric and cytoplasmic pools occurs at the periphery of the sarcomere (Belcastro et al., 1991; Russell et al., 1992) and is the rate-limiting step in the incorporation of newly-synthesized protein into the contractile apparatus (Feng et al., 2009). Thus, a high protein turnover rate would facilitate rearrangement of the myofilaments within the myofibril.

Synthesis of soluble and myofibrillar proteins increased during proecdysis (premolt), confirming results from a previous study on *G. lateralis* by Skinner (Skinner, 1965). Skinner observed a 6.5-fold increase in the incorporation of [1-$^{14}$C]leucine into total protein from skeletal muscle during early to mid premolt (pooled samples from stages $D_0$ to $D_2$) that was reversed in late premolt or early postmolt. The present study expands on this work by quantifying protein synthesis in the soluble and myofibrillar protein fractions, and provides a more detailed examination of protein synthesis during stages $D_0$ to $D_2$. The increase in protein synthesis that occurs in atrophic claw muscle peaks during mid to late premolt. During premolt, *de novo* synthesis of myofibrillar and soluble protein in the claw increases approximately 11- and 13-fold, respectively (Fig. 1A; ranging from $R$=20 to 23). Peak values indicate that the rate of protein synthesis may increase as much as 20-fold in both protein pools by late $D_1$ (Fig. 1A). Data presented in Fig. 1 and by Skinner (Skinner, 1965) indicate that protein synthesis reaches a maximum in claw muscle between the late $D_1$ and $D_3$ stages of premolt, and begins to decrease prior to ecdysis. This coincides with a peak in hemolymph ecdysteroids at stage $D_2$ (Skinner, 1985b). The decrease in protein synthesis during late premolt may be regulated by the large drop in circulating ecdysteroids at stage $D_3$ (Skinner, 1985b). Muscle atrophy, and associated remodeling of the contractile apparatus, is completed by this stage (Skinner, 1985b).

The increase in protein synthesis that occurs in atrophic claw muscle appears to involve two distinct phases of regulation. The relationship between protein synthesis in soluble and myofibrillar protein pools changes significantly in late $D_0$ of premolt (Fig. 1B). The relative increase in protein synthetic rate for the two protein pools is nearly equivalent in animals with an R-index of more than 13, but preferential incorporation of [$^{35}$S]methionine into soluble protein occurs in animals with an R-index less than 13 (1.4:1, soluble:myofibrillar ratio; Fig. 1B). Although there is a great deal of evidence indicating that proteolytic systems are upregulated in atrophic claw muscle (reviewed by Goll et al., 2003; Mykles, 1998) (see also Kramerova et al., 2005; Murphy et al., 2007), it is as yet unclear what proteins are preferentially synthesized during early premolt. Whatever the case, it is clear that the preferential incorporation into soluble protein early in premolt must involve many proteins, as there are no obvious changes in the pool of radioactively-labeled proteins during premolt (Fig. 2C).

Increased capacity for protein synthesis during premolt involves an increase in ribosomal RNA content. Levels of rRNA increase by 40% in epidermis, digestive gland and skeletal muscle in *G. lateralis* during premolt (Skinner, 1968). Since copy number was expressed as a function of total RNA, seemingly steady-state levels of an mRNA may actually reflect a nearly 40% increase in abundance during premolt. Given that only one out of five of the transcripts examined decreased during the period when rRNA content in muscle was increasing, it is reasonable to suggest that either a global increase in transcription or a decrease in RNA degradation occurs in skeletal muscle during premolt. Decreased incorporation of [$^3$H]uridine into rRNA in epithelial tissue during premolt suggests that stability of ribosomes increases in this tissue during premolt (Skinner, 1966).

Ecdysteroids may stimulate protein degradation by activating calpains that degrade myofibrillar proteins (for reviews, see Mykles, 1998; Mykles, 1999), but this activation does not appear to involve transcriptional regulation. Levels of *Gl-CalpM* and *Gl-CalpB* mRNA do not change after ESA (Kim et al., 2005a), and, although *Gl-CalpT* mRNA levels increase threefold in atrophic claw muscle during early premolt, transcript levels initially decrease by 40% to 60% after molt induction (Fig. 3F, Fig. 4F). Thus, there is no significant difference between intermolt and premolt (late $D_0$ to $D_2$) levels of *Gl-CalpT* mRNA. These data differ somewhat from that of Kim et al. (Kim et al., 2005a), who reported a transient increase in *Gl-CalpT* mRNA in claw 1 day after ESA. The reason for this discrepancy is not clear. However, given the modest changes in *Gl-CalpT* mRNA levels observed during molt-induced atrophy of the claw (Fig. 3F, Fig. 4F), and the significant decrease in Gl-CalpT mRNA observed during atrophy of thoracic muscle induced by limb autotomy (Fig. 6), we conclude that Gl-CalpT activity is not regulated at the transcriptional level in atrophic crustacean muscle.

Ecdysteroids appear to control *Gl-Mstn* expression in skeletal muscle over much of the molting cycle. *Gl-Mstn* mRNA levels decrease by at least 68% in thoracic muscle and 81% in claw muscle

during premolt (Fig. 3D, Fig. 4D). *Gl-Mstn* transcript abundance in claw muscle is also negatively correlated with ecdysteroid levels over the same period (Fig. 5). The relatively low correlation between hemolymph ecdysteroids and *Gl-Mstn* expression in thoracic muscle may result, in part, from greater suppression at low ecdysteroid levels indicative of intermolt animals; *Gl-Mstn* expression in intermolt animals is 50–60% greater in claw muscle than in thoracic muscle. At 2 days postmolt, when ecdysteroid titers are low, *Gl-Mstn* mRNA levels increase in thoracic and claw muscle by 6- and 10-fold, respectively (Fig. 4D). In view of these data, it seems reasonable to suggest that *Gl-Mstn* is negatively regulated by ecdysteroid during premolt and early postmolt. However, the regulation of *Gl-Mstn* expression also appears to involve ecdysteroid-independent signals. Despite the presence of unchanging and extremely low ecdysteroid levels following ecdysis, *Gl-Mstn* mRNA in thoracic and claw muscles decreases by 57% and 84%, respectively, between 2 days and 10 days postmolt (Fig. 4D). A direct link between ecdysteroid signaling and expression of *Gl-Mstn* remains to be established.

Autotomy-induced muscle atrophy differs from molt-induced atrophy both in its regulatory origin and transcriptional profile. In response to the loss of a limb, the thoracic muscle atrophies rapidly and more than half of the mass is lost; it remains in an atrophied state until a new limb is regenerated and becomes fully functional after molting (Moffett, 1987). However, unlike atrophy of the claw during premolt, atrophy of thoracic muscle in response to limb autotomy does not appear to be regulated by ecdysteroids, as atrophy occurs during intermolt when ecdysteroid levels are low (Fig. 3A, Fig. 4A). The intact innervation and muscle structure (Moffett, 1987) suggests that the mechanism may be a response to physical unweighting. What is clear is that the regulation of *Gl-Mstn* expression differs between molt-induced atrophy and autotomy-induced atrophy of the thoracic muscle. Although Gl-Mstn mRNA decreases as much as 82% in weighted thoracic muscle and 94% in claw muscle during premolt, levels increase by 300% in unweighted thoracic muscles (Fig. 6). Atrophy in unweighted thoracic muscle may be very similar to some forms of disuse atrophy observed in mammals (reviewed by Favier et al., 2008). An interesting question is whether elevated levels of *Gl-Mstn* transcript in unweighted thoracic muscle are correlated with a decrease in global protein synthesis.

The regulation of Mstn expression in crustacean muscles induced by ESA and MLA differs from that in mammalian muscles induced to atrophy by various treatments or conditions. In mammals, *Mstn* mRNA levels are elevated in muscle atrophies induced by diseases (Carneiro et al., 2008; Costelli et al., 2008), denervation (Liu et al., 2007; Shao et al., 2007), unloading (Allen et al., 2009; Reardon et al., 2001; Wehling et al., 2000), glucocorticoid (Ma et al., 2003) and aging (Leger et al., 2008). Glucocorticoids stimulate *Mstn* transcription *via* response elements in the promoter region (Ma et al., 2001) (for reviews, see Schakman et al., 2008; Tisdale, 2009). Glucocorticoids also stimulate protein degradation and inhibit protein synthesis in mammalian skeletal muscles *via* Mstn signaling (for reviews, see Schakman et al., 2008; Tisdale, 2009). Moreover, atrophy induced by dexamethasone is prevented by deletion of the *Mstn* gene in knockout mice (Gilson et al., 2007). By contrast, *Mstn* expression in crustacean muscles is inversely correlated with ecdysteroid levels (Fig. 5), and *Gl-Mstn* mRNA is reduced during molt-induced atrophy (Fig. 3D, Fig. 4D).

Although *Mstn* expression in mammalian and crustacean muscles responds differently to steroid hormones, the data presented here support the hypothesis that Mstn inhibits protein synthesis in both groups of organisms through the target of rapamycin complex 1 (TORC1). TORC1, a component of the insulin/insulin-like growth factor pathway controlling growth in eukaryotic cells and is a serine/threonine protein kinase; it regulates protein synthesis at the translational level through the phosphorylation of S6 kinase and 4EF-binding protein-1 (for reviews, see Proud, 2007; Wullschleger et al., 2006). This same pathway mediates nutrient-dependent growth in insects (for a review, see Mirth and Riddiford, 2007). There is growing recognition that TORC1 is central to the effects of growth factors, nutrients, contraction and aging on mammalian muscle mass (reviewed by Drummond et al., 2009; Miyazaki and Esser, 2009; Sandri, 2008). Recent studies indicate that Mstn is a negative regulator of this pathway in mammalian muscle. Mstn inhibits signaling *via* TORC1 in rat skeletal muscle (Amirouche et al., 2009) and protein synthesis in $C_2C_{12}$ muscle cells (Taylor et al., 2001). Furthermore, Mstn reduces phosphorylation of Akt (McFarlane et al., 2006), which could lead to inactivation of TORC1 (Proud, 2007). Conversely, Mstn inhibition stimulates protein synthesis *via* the TORC1 pathway in mouse skeletal muscle (Welle et al., 2009). In decapod crustaceans, elevated ecdysteroids have only a small effect on gene expression of myofibrillar protein, suggesting that transcriptional regulation has a relatively minor contribution to changes in protein levels occurring over the molting cycle (El Haj, 1999; Medler et al., 2005; Whiteley and El Haj, 1997; Whiteley et al., 1992). However, increased protein synthesis is correlated with increased ribosomal RNA and activity in muscles from premolt animals (El Haj et al., 1996; Skinner, 1968). The downregulation of Gl-Mstn is associated with an increase in global synthesis of both soluble and myofibrillar proteins (Figs 1, 2). Taken together, these data provide evidence to suggest that Gl-Mstn, either directly or indirectly, suppresses protein synthesis. Further studies are needed to establish whether Gl-Mstn inhibits translation *via* TORC1.

For future studies using molt induction, it is relevant to note that an examination of ecdysteroidogenesis and gene expression in skeletal muscle demonstrates that ESA and MLA stimulate similar, but not identical, responses. Both ESA and MLA cause precocious molting, but the two differ in the timing of hormonal cues and premolt processes. ESA triggers an acute response by the Y-organ, resulting in elevated hemolymph ecdysteroid levels within 1 day of ESA and a shortened premolt period (Skinner and Graham, 1972). By contrast, intermolt animals induced by MLA enter premolt 2–3 weeks after the procedure (Holland and Skinner, 1976), and ecdysteroids increase more gradually. Expression of Gl-EcR follows a similar pattern to that reported by Kim et al. (Kim et al., 2005a) during the first 3 days after ESA, wherein a transient increase is observed in claw muscle and a transient decrease is observed in thoracic muscle. Expression of Gl-EcR converges somewhat between these tissues over a period of 2 weeks. By contrast, a consistent increase in *Gl-EcR* mRNA is observed in both claw and thoracic muscle during premolt induced by MLA. In addition, levels of *Gl-RXR* mRNA remain unchanged throughout the molt cycle induced by MLA, but decrease transiently during stage $D_0$ in ESA animals. These data confirm that skeletal muscle is responsive to changes in ecdysteroids over a molting cycle, and that the rate of change in ecdysteroid titers affects the expression of responsive genes, including those for ecdysteroid receptor subunits.

In summary, Gl-Mstn is differentially regulated in two distinct atrophic tissues: premolt claw muscle and unweighted thoracic muscle. The reduction in *Gl-Mstn* transcript in premolt claw and thoracic muscle is correlated with increasing ecdysteroid levels. These data provide support for the hypothesis that ecdysteroids repress *Gl-Mstn* expression during premolt when bound to the

EcR–RXR heterodimer. This is contrary to the prevailing view, which holds that heterodimeric hormone receptors, in the absence of hormone, interact with co-repressors to prevent transcription; ligand binding induces a conformational change that causes dissociation of the corepressors (reviewed by Gurevich et al., 2007). The most parsimonious explanation for these data is that the binding of ecdysteroid allows the receptor to interact with a co-repressor and block transcription of *Gl-Mstn*. To our knowledge gene repression by ecdysteroid binding to nuclear receptors has not been reported in arthropods. Ecdysteroid and ESA downregulate gene expression in crayfish digestive gland (Shechter et al., 2007), but it is not known whether the effects are direct or indirect. However, a number of co-repressors that require ligand binding to nuclear receptors have been reported in mammals (reviewed by Gurevich et al., 2007). Interestingly, low ecdysteroid levels in intermolt animals permit the upregulation of *Gl-Mstn* in unweighted thoracic muscle, but this upregulation is overridden by elevated ecdysteroids during premolt (Fig. 7). We conclude that ecdysteroids repress *Gl-Mstn* expression in both claw and thoracic muscles. The data presented here support the hypothesis that Gl-Mstn functions as an inhibitor of global protein synthesis in crustacean skeletal muscle.

## LIST OF ABBREVIATIONS

| | |
|---|---|
| Calp | calpain ($Ca^{2+}$-dependent protease) |
| EcR | ecdysone receptor |
| EF-2 | eukaryotic elongation factor 2 |
| ESA | eyestalk ablation |
| Gl | *Gecarcinus lateralis* |
| MLA | multiple limb autotomy |
| Mstn | myostatin |
| qRT-PCR | real-time reverse transcription-polymerase chain reaction |
| R-index | regeneration index |
| RXR | retinoid X receptor |

## ACKNOWLEDGEMENTS

This work was supported by grants from the National Science Foundation (IBN-0342982 and IOS-0745224). We thank Hector C. Horta (Puerto Rico Department of Natural and Environmental Resources) for animal collection; Marcy Haire for technical assistance with organ cultures; Sharon Chang for ecdysteroid radioimmunoassay; Staci Amburgey, Linsey Atchinson, Lisa Axtman, Il-Gyu Cho, Peter Exener, Ashley Larson, Katie Regelson and Kristin Van Ort for animal care; and Audrey McDonald and Sere Williams for assistance with limb bud measurements. We are also grateful to Ricardo Colon Alvarez, Vice-minister and Executive Director, and staff of Consejo Dominicano de Pesca Y Acuicultura (CODOPESCA) for facilitating the collection of *G. lateralis*.

## REFERENCES

**Allen, D. L., Bandstra, E. R., Harrison, B. C., Thorng, S., Stodieck, L. S., Kostenuik, P. J., Morony, S., Lacey, D. L., Hammond, T. G., Leinwand, L. L. et al.** (2009). Effects of spaceflight on murine skeletal muscle gene expression. *J. Appl. Physiol.* **106**, 582-595.

**Amirouche, A., Durieux, A. C., Banzet, S., Koulmann, N., Bonnefoy, R., Mouret, C., Bigard, X., Peinnequin, A. and Freyssenet, D.** (2009). Down-regulation of Akt/mammalian target of rapamycin signaling pathway in response to myostatin overexpression in skeletal muscle. *Endocrinology* **150**, 286-294.

**Avruch, J. and Wallach, D. F. H.** (1971). Preparation and properties of plasma membrane and endoplasmic reticulum fragments from isolated rat fat cells. *Biochim. Biophys. Acta* **233**, 334-337.

**Belcastro, A. N., Scrubb, J. and Gilchrist, J. S.** (1991). Regulation of ATP-stimulated releasable myofilaments from cardiac and skeletal muscle myofibrils. *Mol. Cell. Biochem.* **103**, 113-120.

**Bliss, D. E.** (1956). Neurosecretion and the control of growth in a decapod crustacean. In *Bertil Hanstron, Zoological Papers in Honor of His Sixty-fifth Birthday* (ed. K. G. Eingstrand), pp. 56-57. Lund, Sweden: Zool. Inst.

**Bliss, D. E. and Boyer, J. R.** (1964). Environmental regulation of growth in the decapod crustacean *Gecarcinus lateralis*. *Gen. Comp. Endocrinol.* **4**, 15-41.

**Bollum, F. J.** (1968). Filter paper disk techniques for assaying radioactive macromolecules. *Meth. Enzymol.* **12**, 169-173.

**Carneiro, I., Castro-Piedras, I., Munoz, A., Labandeira-Garcia, J. L., Devesa, J. and Arce, V. M.** (2008). Hypothyroidism is associated with increased myostatin expression in rats. *J. Endocrinol. Invest.* **31**, 773-778.

**Costelli, P., Muscaritoli, M., Bonetto, A., Penna, F., Reffo, P., Bossola, M., Bonelli, G., Doglietto, G. B., Baccino, F. M. and Fanelli, F. R.** (2008). Muscle myostatin signalling is enhanced in experimental cancer cachexia. *Eur. J. Clin. Invest.* **38**, 531-538.

**Covi, J., Gomez, A., Chang, S., Lee, K., Chang, E. and Mykles, D.** (2008a). Repression of Y-organ ecdysteroidogenesis by cyclic nucleotides and agonists of NO-sensitive guanylyl cyclase. In *4th Meeting of Comparative Physiologists & Biochemists in Africa - Mara 2008 - "Molecules to Migration: The Pressures of Life"* (ed. S. Morris and A. Vosloo), pp. 37-46. Bologna, Italy: Monduzzi Editore International.

**Covi, J. A., Kim, H. W. and Mykles, D. L.** (2008b). Expression of alternatively spliced transcripts for a myostatin-like protein in the blackback land crab, *Gecarcinus lateralis*. *Comp. Biochem. Physiol.* **150A**, 423-430.

**Drach, P.** (1939). Meu et cycle d'intermue chez les Crustaces Decapodes. *Ann. Inst. Oceanogr.* **19**, 103-391.

**Drummond, M. J., Dreyer, H. C., Fry, C. S., Glynn, E. L. and Rasmussen, B. B.** (2009). Nutritional and contractile regulation of human skeletal muscle protein synthesis and mTORC1 signaling. *J. Appl. Physiol.* **106**, 1374-1384.

**Durieux, A. C., Amirouche, A., Banzet, S., Koulmann, N., Bonnefoy, R., Pasdeloup, M., Mouret, C., Bigard, X., Peinnequin, A. and Freyssenet, D.** (2007). Ectopic expression of myostatin induces atrophy of adult skeletal muscle by decreasing muscle gene expression. *Endocrinology* **148**, 3140-3147.

**El Haj, A. J.** (1999). Regulation of muscle growth and sarcomeric protein gene expression over the intermolt cycle. *Am. Zool.* **39**, 570-579.

**El Haj, A. J., Clarke, S. R., Harrison, P. and Chang, E. S.** (1996). *In vivo* muscle protein synthesis rates in the American lobster *Homarus americanus* during the moult cycle and in response to 20-hydroxyecdysone. *J. Exp. Biol.* **199**, 579-585.

**Favier, F. B., Benoit, H. and Freyssenet, D.** (2008). Cellular and molecular events controlling skeletal muscle mass in response to altered use. *Eur. J. Physiol.* **456**, 587-600.

**Feng, H. Z., Hossain, M. M., Huang, X. P. and Jin, J. P.** (2009). Myofilament incorporation determines the stoichiometry of troponin I in transgenic expression and the rescue of a null mutation. *Arch. Biochem. Biophys.* **487**, 36-41.

**Festuccia, W. T., Laplante, M., Brule, S. V. P. H., Achouba, A., Lachance, D., Pedrosa, M. L., Silva, M. E., Guerra-Sa, R., Couet, J., Arsenault, M. et al.** (2009). Rosiglitazone-induced heart remodelling is associated with enhanced turnover of myofibrillar protein and mTOR activation. *J. Mol. Cell. Cardiol.* **47**, 85-95.

**Gilson, H., Schakman, O., Combaret, L., Lause, P., Grobet, L., Attaix, D., Ketelslegers, J. M. and Thissen, J. P.** (2007). Myostatin gene deletion prevents glucocorticoid-induced muscle atrophy. *Endocrinology* **148**, 452-460.

**Goll, D. E., Thompson, V. F., Li, H. Q., Wei, W. and Cong, J. Y.** (2003). The calpain system. *Physiol. Rev.* **83**, 731-801.

**Gurevich, I., Flores, A. M. and Aneskievich, B. J.** (2007). Corepressors of agonist-bound nuclear receptors. *Toxicol. Appl. Pharmacol.* **223**, 288-298.

**Herpin, A., Lelong, C. and Favrel, P.** (2004). Transforming growth factor-beta-related proteins: an ancestral and widespread superfamily of cytokines in metazoans. *Dev. Comp. Immunol.* **28**, 461-485.

**Holland, C. A. and Skinner, D. M.** (1976). Interactions between molting and regeneration in the land crab. *Biol. Bull.* **150**, 222-240.

**Hopkins, P. M.** (1993). Regeneration of walking legs in the fiddler crab *Uca pugilator*. *Am. Zool.* **33**, 348-356.

**Ismail, S. Z. M. and Mykles, D. L.** (1992). Differential molt-induced atrophy in the dimorphic claws of male fiddler crabs, *Uca pugnax*. *J. Exp. Zool.* **263**, 18-31.

**Kim, H. W., Batista, L. A., Hoppes, J. L., Lee, K. J. and Mykles, D. L.** (2004). A crustacean nitric oxide synthase expressed in nerve ganglia, Y-organ, gill and gonad of the tropical land crab, *Gecarcinus lateralis*. *J. Exp. Biol.* **207**, 2845-2857.

**Kim, H. W., Chang, E. S. and Mykles, D. L.** (2005a). Three calpains and ecdysone receptor in the land crab, *Gecarcinus lateralis*: sequences, expression, and effects of elevated ecdysteroid induced by eyestalk ablation. *J. Exp. Biol.* **208**, 3177-3197.

**Kim, H. W., Lee, S. G. and Mykles, D. L.** (2005b). Ecdysteroid-responsive genes, RXR and E75, in the tropical land crab, *Gecarcinus lateralis*: Differential tissue expression of multiple RXR isoforms generated at three alternative splicing sites in the hinge and ligand-binding domains. *Mol. Cell. Endocrinol.* **242**, 80-95.

**Kramerova, I., Kudryashova, E., Venkatraman, G. and Spencer, M. J.** (2005). Calpain 3 participates in sarcomere remodeling by acting upstream of the ubiquitin-proteasome pathway. *Human Mol. Genetics* **14**, 2125-2134.

**Lee, S. J.** (2004). Regulation of muscle mass by myostatin. *Ann. Rev. Cell Dev. Biol.* **20**, 61-86.

**Leger, B., Derave, W., De Bock, K., Flespel, P. and Russell, A. P.** (2008). Human sarcopenia reveals an increase in SOCS-3 and myostatin and a reduced efficiency of akt phosphorylation. *Rejuvenation Res.* **11**, 163-175.

**Liu, F.** (2003). Receptor-regulated Smads in TGF-beta signaling. *Front. Biosci.* **8**, S1280-S1303.

**Liu, M., Zhang, D. L., Shao, C. X., Liu, M., Ding, F. and Gu, X. S.** (2007). Expression pattern of myostatin in gastrocnemius muscle of rats after sciatic nerve crush injury. *Muscle Nerve* **35**, 649-656.

**Ma, K., Mallidis, C., Artaza, J., Taylor, W., Gonzalez-Cadavid, N. and Bhasin, S.** (2001). Characterization of 5 '-regulatory region of human myostatin gene: regulation by dexamethasone *in vitro*. *Am. J. Physiol.* **281**, E1128-E1136.

**Ma, K., Mallidis, C., Bhasin, S., Mahabadi, V., Artaza, J., Gonzalez-Cadavid, N., Arias, J. and Salehian, B.** (2003). Glucocorticoid-induced skeletal muscle atrophy is associated with upregulation of myostatin gene expression. *Am. J. Physiol.* **285**, E363-E371.

**Magee, T. R., Artaza, J. N., Ferrini, M. G., Vernet, D., Zuniga, F. I., Cantini, L., Reisz-Porszasz, S., Rajfer, J. and Gonzalez-Cadavid, N. F.** (2006). Myostatin short interfering hairpin RNA gene transfer increases skeletal muscle mass. *J. Gene Med.* **8**, 1171-1181.

**Matsakas, A. and Patel, K.** (2009). Intracellular signalling pathways regulating the adaptation of skeletal muscle to exercise and nutritional changes. *Histol. Histopathol.* **24**, 209-222.

**McFarlane, C., Plummer, E., Thomas, M., Hennebry, A., Ashby, M., Ling, N., Smith, H., Sharma, M. and Kambadur, R.** (2006). Myostatin induces cachexia by activating the ubiquitin proteolytic system through an NF-kappa B-independent, FoxO1-dependent mechanism. *J. Cell. Physiol.* **209**, 501-514.
**Medeiros, E. F., Phelps, M. P., Fuentes, F. D. and Bradley, T. M.** (2009). Over expression of follistatin in trout stimulates increased muscling. *Am. J. Physiol.* **297**, R235-R242.
**Medler, S., Brown, K. J., Chang, E. S. and Mykles, D. L.** (2005). Eyestalk ablation has little effect on actin and myosin heavy chain gene expression in adult lobster skeletal muscles. *Biol. Bull.* **208**, 127-137.
**Medler, S., Lilley, T. R., Riehl, J. H., Mulder, E. P., Chang, E. S. and Mykles, D. L.** (2007). Myofibrillar gene expression in differentiating lobster claw muscles. *J. Exp. Zool.* **307A**, 281-295.
**Mirth, C. K. and Riddiford, L. M.** (2007). Size assessment and growth control: how adult size is determined in insects. *BioEssays* **29**, 344-355.
**Miyazaki, M. and Esser, K. A.** (2009). Cellular mechanisms regulating protein synthesis and skeletal muscle hypertrophy in animals. *J. Appl. Physiol.* **106**, 1367-1373.
**Moffett, S.** (1987). Muscles proximal to the fracture plane atrophy after limb autotomy in decapod crustaceans *J. Exp. Zool.* **244**, 485-490.
**Murphy, R. M., Goodman, C. A., McKenna, M. J., Bennie, J., Leikis, M. and Lamb, G. D.** (2007). Calpain-3 is autolyzed and hence activated in human skeletal muscle 24 h following a single bout of eccentric exercise. *J. Appl. Physiol.* **103**, 926-931.
**Mykles, D. L.** (1990). Calcium-dependent proteolysis in crustacean claw closer muscle maintained *in vitro*. *J. Exp. Zool.* **256**, 16-30.
**Mykles, D. L.** (1997). Crustacean muscle plasticity: Molecular mechanisms determining mass and contractile properties. *Comp. Biochem. Physiol.* **117B**, 367-378.
**Mykles, D. L.** (1998). Intracellular proteinases of invertebrates: calcium-dependent and proteasome/ubiquitin-dependent systems. *Int. Rev. Cytol.* **184**, 157-289.
**Mykles, D. L.** (1999). Proteolytic processes underlying molt-induced claw muscle atrophy in decapod crustaceans. *Am. Zool.* **39**, 541-551.
**Mykles, D. L.** (2001). Interactions between limb regeneration and molting in decapod crustaceans. *Am. Zool.* **41**, 399-406.
**Mykles, D. L. and Skinner, D. M.** (1981). Preferential loss of thin filaments during molt-induced atrophy in crab claw muscle. *J. Ultrastruct. Res.* **75**, 314-325.
**Mykles, D. L. and Skinner, D. M.** (1982a). Crustacean muscles: atrophy and regeneration during molting. In *Basic Biology of Muscles: A Comparative Approach* (ed. B. M. Twarog R. J. C. Levine and M. M. Dewey), pp. 337-357. New York: Raven Press.
**Mykles, D. L. and Skinner, D. M.** (1982b). Molt cycle-associated changes in calcium-dependent proteinase activity that degrades actin and myosin in crustacean muscle. *Dev. Biol.* **92**, 386-397.
**Nakatani, M., Takehara, Y., Sugino, H., Matsumoto, M., Hashimoto, O., Hasegawa, Y., Murakami, T., Uezumi, A., Takeda, S., Noji, S. et al.** (2008). Transgenic expression of a myostatin inhibitor derived from follistatin increases skeletal muscle mass and ameliorates dystrophic pathology in mdx mice. *FASEB J.* **22**, 477-487.
**O'Brien, J. J., Mykles, D. L. and Skinner, D. M.** (1986). Cold-induced apolysis in anecdysial brachyurans. *Biol. Bull.* **171**, 450-460.
**Proud, C. G.** (2007). Signalling to translation: how signal transduction pathways control the protein synthetic machinery. *Biochem. J.* **403**, 217-234.
**Qiao, C. P., Li, J. B., Jiang, J. G., Zhu, X. D., Wang, B., Li, J. and Xiao, X.** (2008). Myostatin propeptide gene delivery by adeno-associated virus serotype 8 vectors enhances muscle growth and ameliorates dystrophic phenotypes in mdx mice. *Human Gene Therapy* **19**, 241B-254B.
**Reardon, K. A., Davis, J., Kapsa, R. M. I., Choong, P. and Byrne, E.** (2001). Myostatin, insulin-like growth factor-1, and leukemia inhibitory factor mRNAs are upregulated in chronic human disuse muscle atrophy. *Muscle Nerve* **24**, 893-899.
**Reisz-Porszasz, S., Bhasin, S., Artaza, J. N., Shen, R. Q., Sinha-Hikim, I., Hogue, A., Fielder, T. J. and Gonzalez-Cadavid, N. F.** (2003). Lower skeletal muscle mass in male transgenic mice with muscle-specific overexpression of myostatin. *Am. J. Physiol.* **285**, E876-E888.
**Rodgers, B. D. and Garikipati, D. K.** (2008). Clinical, agricultural, and evolutionary biology of myostatin: A comparative review. *Endocrine Rev.* **29**, 513-534.
**Russell, B., Wenderoth, M. P. and Goldspink, P. H.** (1992). Remodeling of myofibrils: Subcellular distribution of myosin heavy chain mRNA and protein. *Am. J. Physiol.* **262**, R339-R345.
**Sandri, M.** (2008). Signaling in muscle atrophy and hypertrophy. *Physiology* **23**, 160-170.
**Schakman, O., Gilson, H. and Thissen, J. P.** (2008). Mechanisms of glucocorticoid-induced myopathy. *J. Endocrinol.* **197**, 1-10.
**Schmiege, D. L., Ridgway, R. L. and Moffett, S. B.** (1992). Ultrastructure of autotomy-induced atrophy of muscles in the crab *Carcinus maenas*. *Can. J. Zool.* **70**, 841-851.
**Shao, C. X., Liu, M., Wu, X. and Ding, F.** (2007). Time-dependent expression of myostatin RNA transcript and protein in gastrocnemius muscle of mice after sciatic nerve resection. *Microsurgery* **27**, 487-493.
**Shechter, A., Tom, M., Yudkovski, Y., Weil, S., Chang, S. A., Chang, E. S., Chalifa-Caspi, V., Berman, A. and Sagi, A.** (2007). Search for hepatopancreatic ecdysteroid-responsive genes during the crayfish molt cycle: from a single gene to multigenicity. *J. Exp. Biol.* **210**, 3525-3537.
**Skinner, D. M.** (1962). The structure and metabolism of a crustacean integumentary tissue during a molt cycle. *Biol. Bull.* **123**, 635-647.
**Skinner, D. M.** (1965). Amino acid incorporation into protein during the molt cycle of the land crab, *Gecarcinus lateralis*. *J. Exp. Zool.* **160**, 225-234.
**Skinner, D. M.** (1966). Macromolecular changes associated with growth of crustacean tissues. *Am. Zool.* **6**, 235-242.
**Skinner, D. M.** (1968). Isolation and characterization of ribosomal ribonucleic acid from crustacean, *Gecarcinus lateralis*. *J. Exp. Zool.* **169**, 347-356.
**Skinner, D. M.** (1985a). Interacting factors in the control of the crustacean molt cycle. *Am. Zool.* **25**, 275-284.
**Skinner, D. M.** (1985b). Molting and regeneration. In *The Biology of Crustacea* (ed. D. E. Bliss and L. H. Mantel), pp. 43-146. New York: Academic Press.
**Skinner, D. M. and Graham, D. E.** (1972). Loss of limbs as a stimulus to ecdysis in Brachyura (true crabs). *Biol. Bull.* **143**, 222-233.
**Taylor, W. E., Bhasin, S., Artaza, J., Byhower, F., Azam, M., Willard, D. H., Jr, Kull, F. C., Jr and Gonzalez-Cadavid, N.** (2001). Myostatin inhibits cell proliferation and protein synthesis in $C_2C_{12}$ muscle cells. *Am. J. Physiol.* **280**, E221-E228.
**Termin, A. and Pette, D.** (1992). Changes in myosin heavy-chain isoform synthesis of chronically stimulated rat fast-twitch muscle. *Eur. J. Biochem.* **204**, 569-573.
**Tisdale, M. J.** (2009). Mechanisms of cancer cachexia. *Physiol. Rev.* **89**, 381-410.
**Wehling, M., Cai, B. Y. and Tidball, J. G.** (2000). Modulation of myostatin expression during modified muscle use. *FASEB J.* **14**, 103-110.
**Welle, S., Burgess, K. and Mehta, S.** (2009). Stimulation of skeletal muscle myofibrillar protein synthesis, p70 S6 kinase phosphorylation, and ribosomal protein S6 phosphorylation by inhibition of myostatin in mature mice. *Am. J. Physiol.* **296**, E567-E572.
**Whiteley, N. M. and El Haj, A. J.** (1997). Regulation of muscle gene expression over the moult in Crustacea. *Comp. Biochem. Physiol.* **117B**, 323-331.
**Whiteley, N. M., Taylor, E. W. and El Haj, A. J.** (1992). Actin gene expression during muscle growth in *Carcinus maenas*. *J. Exp. Biol.* **167**, 277-284.
**Wullschleger, S., Loewith, R. and Hall, M. N.** (2006). TOR signaling in growth and metabolism. *Cell* **124**, 471-484.
**Xu, L.** (2006). Regulation of Smad activities. *Biochim. Biophys. Acta* **1759**, 503-513.
**Yu, X. L., Chang, E. S. and Mykles, D. L.** (2002). Characterization of limb autotomy factor-proecdysis ($LAF_{pro}$), isolated from limb regenerates, that suspends molting in the land crab *Gecarcinus lateralis*. *Biol. Bull.* **202**, 204-212.
**Zimmers, T. A., Davies, M. V., Koniaris, L. G., Haynes, P., Esquela, A. F., Tomkinson, K. N., McPherron, A. C., Wolfman, N. M. and Lee, S. J.** (2002). Induction of cachexia in mice by systemically administered myostatin. *Science* **296**, 1486-1488.